Multichannel liquid-crystal-based wave-front corrector with modal influence functions

Alexander F. Naumov

P. N. Lebedev Physical Institute of the Russian Academy of Science, Samara Branch, Novo-Sadovaya Street 221, 443011 Samara, Russia

Gleb Vdovin

Electronic Instrumentation, Technical University of Delft, P.O. Box 5031, 2600 GA Delft, The Netherlands

Received April 21, 1998

We report on a multichannel liquid-crystal-based wave-front corrector with smooth modal influence functions. The phase is controlled by application of spatially localized ac voltages to a distributed voltage divider formed by a liquid-crystal layer sandwiched between a high-conductance and a low-conductance electrode. The shape of the influence function depends on the control frequency and material parameters of the distributed voltage divider. We have experimentally realized a reflective modulator controlled by an array of 16×16 electrodes, providing phase control with an amplitude of $\sim 16\pi$ at $\lambda = 633$ nm with a time constant of the order of tens of milliseconds. We experimentally demonstrated that the amplitude of each influence function can be controlled by change of the control voltage, whereas the width of the influence function is controlled by the frequency of the control voltage in a range of ~ 1 mm to the full width of the modulator aperture. © 1998 Optical Society of America

OCIS codes: 010.7350, 110.1220.

Liquid-crystal- (LC-) based multichannel wave-front correctors present an attractive alternative to traditional deformable mirrors.[1] The vast majority of multichannel LC correctors realize the zonal correction principle through electrical[2,3] or optical[4] addressing, providing a constant pistonlike phase shift over an entire actuated area. The required phase profile is formed as a superposition of zonal piston functions. Pistonlike response complicates phase control[5]; moreover, modal correctors[1,6,7] provide much better correction for smooth and continuous aberrations than do pistonlike zonal correctors with the same number of degrees of freedom. We suggest a new principle of modal control in a multichannel LC phase corrector.

The design of a reflective multichannel phase corrector is illustrated in Fig. 1. A layer of nematic LC is sandwiched between two conductive electrodes. The front transparent electrode, deposited upon the inner side of the transparent glass window, has high electrical conductivity. This electrode is connected to ground. The second electrode has low electrical conductivity. Control actuators are represented by pointlike contacts integrated into the high-resistance electrode. To make the device reflective we deposit a dielectric mirror onto the high-resistance electrode. Appropriate alignment layers (parallel to each other) are deposited as top layers upon both electrodes.

Let us consider the distribution of ac voltage applied to an arbitrary electrode. The active impedance R of the high-resistance electrode, the conductivity G, and the capacitance C of the sandwiched LC layer form a distributed voltage divider. All material parameters are normalized to the unit square S. The material parameters of the LC layer are complex functions of control voltage; moreover, the conductivity G depends on the control frequency: $G = wG_a(U)$, where $G_a(U)$ is the LC conductivity per unit frequency. To simplify the analysis further we take the material parameters to be constant. Applying Kirchhoff's law to the distributed voltage divider formed by the LC layer and the two electrodes, we obtain a differential equation for voltage distribution:

$$\nabla_S{}^2 U = RC \frac{\partial U}{\partial t} + RGU . \tag{1}$$

The field in the vicinity of a highly conductive actuator with a radius r_0 has an axial symmetry; therefore the azimuthal field dependence can be eliminated from Eq. (1) and the equation can be converted into the Bessel form for harmonic voltage amplitude $U \exp(i\omega t)$:

$$\frac{\mathrm{d}^2 U}{\mathrm{d}r^2} + \frac{1}{r}\frac{\mathrm{d}U}{\mathrm{d}r} - \chi^2 U = 0 , \tag{2}$$

where $\chi^2 = R\omega(G_a + iC)$. To solve Eq. (1) we have to take into account the boundary conditions

$$U|_{r \le r_0} = U_0 , \qquad \frac{\mathrm{d}U}{\mathrm{d}r}|_{r=l} = 0 , \tag{3}$$

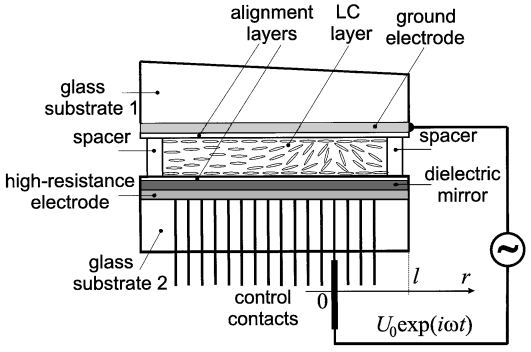

Fig. 1. Schematic diagram of a multichannel reflective LC phase corrector.

0146-9592/98/191550-03$15.00/0

where l is the distance to the edge of modulator aperture. The exact solution of Eq. (2) has the form

$$U(r) = U_0 \frac{K_1(\chi l)I_0(\chi r) + I_1(\chi l)K_0(\chi r)}{K_0(\chi r_0)I_1(\chi l) + K_1(\chi l)I_0(\chi r_0)}. \quad (4)$$

It follows from analysis of Eq. (4) that the voltage distribution will be localized in the vicinity of the control electrode at high values of $|\chi|$ that correspond to high frequencies of ac control voltage and will be distributed over the entire area of the LC cell at low values of $|\chi|$ corresponding to low control frequencies.

The electro-optical response of the LC $\Delta\Phi(U)$ measured interferometrically at low control frequency, which provides constant phase delay over the entire area of the LC modulator, is shown in Fig. 2. In a further analysis we used a normalized analytical approximation of this measured characteristic.

The solutions of Eq. (4) tabulated for three values of $|\chi|$ are shown in Fig. 3. Solid curves correspond to distributions of the voltage $U(r)$; dashed curves illustrate the phase difference between the nonordinary and the ordinary waves $\Delta\Phi[U(r)]$. This delay is zero when the maximum voltage is applied, opposite the notation accepted in adaptive optics (zero delay when zero voltage is applied). Figure 3 illustrates the possibility of controlling the width of the influence function by changing the frequency of the control voltage.

Nonlinearity of the electro-optical response $\Delta\Phi(U)$ provides for yet another possibility to control the width of the influence function. When the voltage is high, the phase delay saturates in the area about the actuator, extending the wings of the influence function, which is equivalent to a widening of the saturated influence function.

In our experiments we used a LC modulator (see Fig. 4) based on the electro-optical S effect formed by a 12-μm-thick layer of nematic LC with a birefringence $\Delta n = 0.21$ at $\lambda = 633$ nm. The low-resistance transparent electrode was formed by an indium tin oxide film, and the high-resistance electrode was formed by evaporation of a composition of Ni:Fe:Si coated by a 19-layer dielectric mirror optimized for $\lambda = 553$ nm. The electrode structure consisted of an array of 16×16 electrodes positioned in a rectangular grid with a 1.3-mm center-to center distance. The high-resistance layer provided for a resistance of $\sim$20 kΩ between adjacent electrodes.

Interferometric patterns registered by a Twyman–Green interferometer with a flat reference in plane-polarized light with $\lambda = 633$ nm are shown in Fig. 5. Variation of the frequency of the control voltage with a constant peak-to-peak amplitude $U_0 = 7.5$ V applied to a single actuator causes variation of the width of the influence function from a nearly uniform phase shift over the entire area of the modulator at a frequency of 10 kHz to a sharp influence function localized in an area with a diameter to $\sim$1 mm at 1 MHz. Higher conductivity of the LC layer at high frequencies owing to the dispersion of the LC dielectric constant sharpens the influence function even more. The amplitude of the influence function is preserved in the whole range of variation of the control frequency. The possibility of controlling the width and the amplitude of the influence function independently in the quasi-linear region of the electro-optical response curve (2.9–7.5 V in our case) provides an additional degree of freedom in optimization of the modulator parameters.

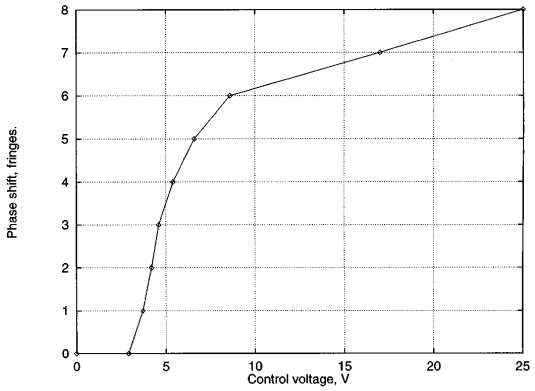

Fig. 2. Experimentally measured electro-optical characteristics of the LC cell.

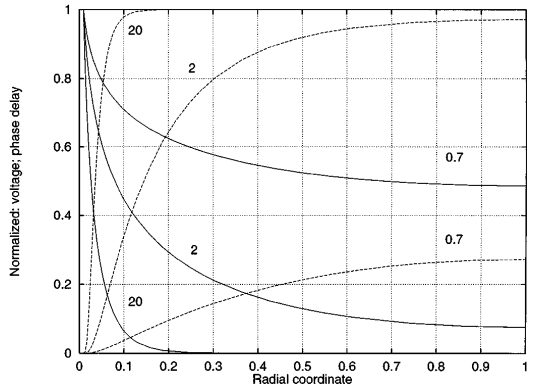

Fig. 3. Calculated normalized voltage distributions (solid curves) and phase delays (dashed curves) for three values of $|\chi|$.

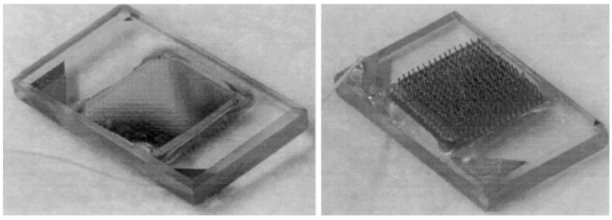

Fig. 4. Front and back views of the 16×16 LC modulator.

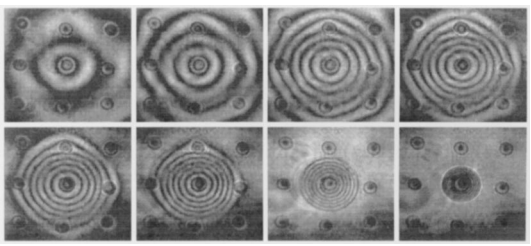

Fig. 5. Influence functions at constant control voltage $U_0 = 7.5$ V and several control frequencies: 10, 20, 50, and 100 kHz (top, left to right) and 150 kHz, 250 kHz, 500 kHz, and 1 MHz (bottom, left to right). At low frequencies the influence function is so wide that only the central fringes are visible in the interferogram.

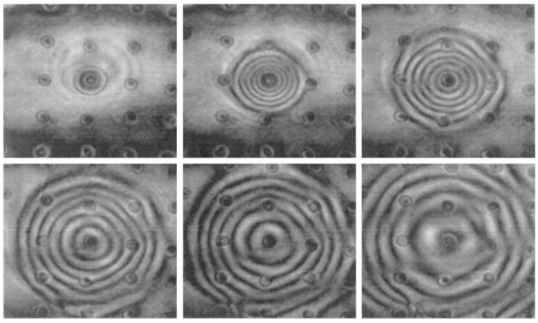

Fig. 6. Influence functions at a control frequency at 75 kHz at several control voltages: 5, 7.5, and 10 V (top, left to right) and 12.5, 15, and 20 V (bottom, left to right).

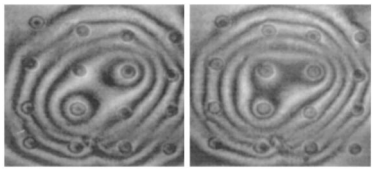

Fig. 7. Superposition of two (left) and three (right) influence functions.

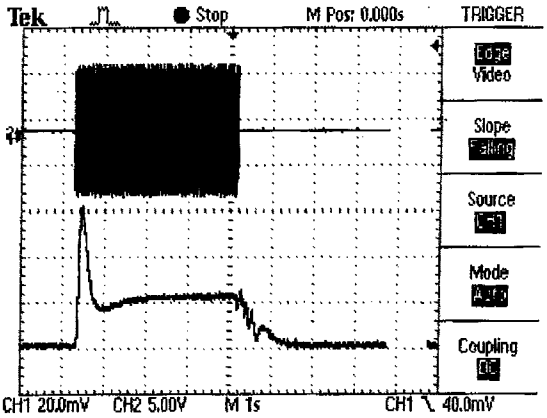

Fig. 8. Optically measured large-signal response (bottom curve) of the LC modulator to a 17.5-V (peak to peak) 75-kHz control voltage applied to a single actuator (top curve).

The second way to control the width of the influence function at a fixed control frequency based on the saturation of electro-optical response $\Delta\Phi(U)$ is illustrated by the experimentally recorded interferograms shown in Fig. 6. The central part of the phase influence function saturates when the control voltage is higher than 10 V. Further increase of the control voltage flattens the top of the influence function and extends the area of function localization.

Figure 7 illustrates the superposition of two and three influence functions. The resultant response is influenced by the nonlinearity of the electro-optical response, which is common to all LC phase modulators. One can linearize the control by storing the measured electro-optical response of the modulator in computer memory and introducing appropriate corrections to the amplitudes of the control signals.

The response of the modulator in an arbitrary point of its aperture can also be influenced by destructive interference of ac electric fields produced by several electrodes. The large phase shifts that lead to the destructive interference are possible only at large values of signal attenuation in the peripheral regions of influence functions. As the LC modulator is not sensitive to any signal attenuated to a value that is lower than 2.9 V (see Fig. 2), we did not observe any interference of cophased ac control signals 2.9–7.5 V in the frequency range 10 kHz to 1 MHz.

The temporal response of the LC modulator was measured by a photodiode with a small aperture in the near-field zone of the light beam reflected from the modulator. The photodiode registers the geometrical modulation of the light intensity produced by the induced focusing power after the control voltage is applied to the actuator. A typical oscillogram for the case of a large control signal is shown in Fig. 8. The bottom curve in Fig. 8 is inverted, so higher values correspond to low illumination of the photodiode. The peak drop of intensity on the front of the pulse is caused by dynamic scattering in the LC layer at the moment of switching on. One can avoid this scattering by biasing the actuator to the beginning of the linear area of electro-optical characteristics. In general the dynamics of response is a complex nonlinear function of the amplitude of control voltage[8]: In our experiments we observed switching times of the order of hundreds of milliseconds from zero to full amplitude for large control signals to ~20 ms for low-amplitude control signals applied to biased LC's.

The corrector can be used only with linearly polarized light. To extend the functionality to an arbitrary state of light polarization one should use two correctors with orthogonally oriented LC layers.

The reported technology provides smooth and continuous response functions, significantly extending the possibilities of LC-based dynamic compensation for continuous random phase aberrations. Moreover, the frequency control in the linear region of the electro-optical curve allows for optimal choice of the influence function's geometry and cross talk, providing additional degrees of freedom.

References

1. R. H. Freeman and J. E. Pearson, Appl. Opt. **21,** 580 (1982).
2. G. D. Love, Appl. Opt. **36,** 1517 (1997).
3. Z. Zhang, G. Lu, and F. T. Yu, Opt. Eng. **33,** 3018 (1994).
4. A. A. Vasil'ev, M. A. Vorontsov, A. V. Korjabin, A. F. Naumov, and V. I. Shmal'gauzen, Sov. J. Quantum Electron. **16,** 599 (1989).
5. J. Gonglewski, S. Brownie, S. Rogers, and S. McDermott, Opt. Express **1,** 338 (1997); www.osa.org.
6. A. F. Naumov, M. Yu. Loktev, I. R. Guralnik, and G. V. Vdovin, Opt. Lett. **23,** 992 (1998).
7. G. Vdovin, S. Middelhoek, and P. M. Sarro, Opt. Eng. **36,** 1382 (1997).
8. U. Efron, S. T. Wu, and T. D. Bates, J. Opt. Soc. Am. B **3,** 247 (1986).